

# **Studying the Effect of Chlorine Introduction in Perovskite through Various Routes and Fabrication of Perovskite Solar Cell**



A thesis submitted in partial fulfilment of requirements for the BS-MS dual degree program (2015 - 2020)

Submitted by

**Keshav Kumar Yadav**

**20151131**

Indian Institute of Science Education and Research, Pune

Under the guidance of

**Dr. Sandeep Pathak**

Assistant Professor

Centre for Energy Studies (CES)

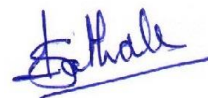
Indian Institute of Technology- Delhi

## CERTIFICATE

This is to certify that this dissertation entitled “Studying the Effect of Chlorine Introduction in Perovskite Through Various Routes and Fabrication of Perovskite Solar Cells” towards the partial fulfilment of the BS-MS dual degree programme at the Indian Institute of Science Education and Research (IISER), Pune represents the work carried out by Keshav Kumar Yadav at Indian Institute of Technology- Delhi (IIT-D) under the supervision of Dr. Sandeep Pathak, Assistant Professor, Centre of Energy Studies, IIT- Delhi during the academic year 2019-2020.



Keshav Kumar Yadav  
Reg no: 20151131  
BS-MS Student  
IISER Pune



Dr. Sandeep Pathak  
Assistant Professor  
CES Department  
IIT- Delhi

## DECLARATION

I hereby declare that the matter embodied in the thesis entitled “Studying the Effect of Chlorine Introduction in Perovskite Through Various Routes and Fabrication of Perovskite Solar Cells” are the results of the work carried out by me at the Centre for Energy Studies, IIT- Delhi, under the supervision of Dr. Sandeep Pathak, Assistant Professor, Centre of Energy Studies, IIT- Delhi and the same has not been submitted elsewhere for any other degree.



Keshav Kumar Yadav  
Reg no: 20151131  
BS-MS Student  
IISER Pune



Dr. Sandeep Pathak  
Assistant Professor  
CES Department  
IIT- Delhi

## ACKNOWLEDGEMENTS

I would like to express my deepest appreciation to Dr. Sandeep Pathak under whose guidance and supervision I was able to undertake this project. He has been a great mentor and an inspiring guide throughout the year. Without his guidance and persistent help, this dissertation would not be possible. Apart from teaching me lab skills and work ethics, he has continuously helped me become a better and stronger person in life.

I would also like to thank my thesis advisor, Dr. Shabana Khan, for her valuable suggestions and comments during my thesis.

I would like to thank my lab members, who helped build a healthy and nurturing work environment in the lab.

I would also like to thank my family including grandparents, mother, father, uncle, aunt, brother, cousins and Dipika for continually encouraging and being there for me whenever I needed it and for pushing me to give my best.

I would like to express my gratitude to Centre for Energy Studies at IIT- Delhi for providing me facilities to carry out my project. I am also thankful to Nanoscale Research Facility (NRF) and Central Research Facility (CRF), the characterisation department at IIT- Delhi.

## ABBREVIATIONS

PL	Photoluminescence
XRD	X- Ray diffraction
PV	Photovoltaic
SEM	Scanning electron microscope
EDX	Energy dispersive spectroscopy
FF	Fill factor
FTO	Fluorine doped tin oxide
PCE	Power conversion efficiency
MAI	Methyl ammonium iodide
Isc	Short circuit current
FAI	Formamidinium iodide
Voc	Open circuit voltage
MAPbI <sub>3</sub>	Methyl ammonium lead tri iodide
FACsPbI <sub>3</sub>	Formamidinium caesium lead tri iodide
MACl	Methyl ammonium chloride
FACl	Formamidine hydrochloride
HCl	Hydrochloric acid
CsI	Caesium iodide
CsCl	Caesium chloride
c-TiO <sub>2</sub>	Compact titanium dioxide
Pb(Ac) <sub>2</sub>	Lead acetate
CB	Chlorobenzene
DMF	Dimethylformamide
DMSO	Dimethyl sulfoxide
IPA	Isopropyl alcohol
ETL	Electron transport layer
HTL	Hole transport layer
RH	Room humidity
RPM	Rotation per minute

# CONTENTS

Certificate.....	02
Declaration .....	03
Acknowledgement.....	04
Abbreviations.....	05
List of Figures.....	07
List of Tables.....	09
Abstract.....	10
1. Introduction.....	11
1.1. Solar cell history.....	13
1.2. Generation of solar cells.....	13
1.3. What are perovskites?.....	16
1.4. Properties of perovskite.....	17
2. Characterization Techniques.....	20
3. Device Fabrication.....	25
3.1. Device physics of solar cell.....	25
3.2. Method and experimental details.....	25
3.3. Result and discussion.....	32
4. Studying the effect of chlorine introduction in perovskite.....	36
4.1. Methods and experimental details.....	36
4.2. Result and discussion.....	38
5. Conclusion.....	45
6. References.....	46

## LIST OF FIGURES

Figure 01. Cell efficiency chart.....	12
Figure 02. Monocrystalline Cell.....	13
Figure 03. Polycrystalline Cell.....	13
Figure 04. Amorphous Silicon cells.....	14
Figure 05. Flexible CdTe Cells.....	14
Figure 06. Flexible CIGS cells.....	14
Figure 07. Organic Solar Cell.....	15
Figure 08. Perovskite crystal structure of the form $ABX_3$ .....	17
Figure 09. Absorption coefficient of PV materials.....	18
Figure 10. Energy bandgap of different materials.....	19
Figure 11. Principle of photoluminescence spectroscopy.....	20
Figure 12. Instrumental setup of SHIMADZU spectrofluorometer.....	20
Figure 13. Instrumental setup of Olympus DP73.....	21
Figure 14. Instrumental set up of XRD.....	22
Figure 15. Instrumental setup of UV-Vis Spectrophotometer.....	23
Figure 16. Instrumental setup of I-V Measurement.....	24
Figure 17. The schematic sketch of a perovskite solar cell and its working.....	26
Figure 18. Steps involved in perovskite device fabrication.....	29
Figure 19. Shifting of I-V curve.....	30
Figure 20. Solar cell I-V curve and its parameters.....	30
Figure 21. SEM image of c-TiO <sub>2</sub> .....	32
Figure 22. Optical of MAPbI <sub>3</sub> .....	32

Figure 23. Optical of FACsPb(I <sub>0.83</sub> Br <sub>0.17</sub> ) <sub>3</sub> .....	32
Figure 24. SEM of MAPbI <sub>3</sub> .....	33
Figure 25. SEM of FACsPb(I <sub>0.83</sub> Br <sub>0.17</sub> ) <sub>3</sub> .....	33
Figure 26. PL of MAPbI <sub>3</sub> .....	33
Figure 27. PL of FACsPb(I <sub>0.83</sub> Br <sub>0.17</sub> ) <sub>3</sub> .....	33
Figure 28. XRD of MAPbI <sub>3</sub> and FACsPb(I <sub>0.83</sub> Br <sub>0.17</sub> ) <sub>3</sub> .....	34
Figure 29. J-V curve of MAPbI <sub>3</sub> .....	34
Figure 30. J-V curve of FACsPb(I <sub>0.83</sub> Br <sub>0.17</sub> ) <sub>3</sub> .....	34
Figure 31. Comparison of optical images in different humidity.....	38
Figure 32. Comparison of PL in different humidity.....	39
Figure 33. SEM images of perovskite films.....	40
Figure 34. XRD plot.....	41
Figure 35. UV-Vis absorption in the visible region.....	42
Figure 36. J-V Curve.....	43



## LIST OF TABLES

Table 1. PV parameters of the MAPbI <sub>3</sub> .....	35
Table 2. PV parameters of the FACsPb(I <sub>0.83</sub> Br <sub>0.17</sub> ) <sub>3</sub> .....	35
Table 3. Elemental analysis of the perovskite films.....	42
Table 4. PV parameters of the FACsPbI <sub>3</sub> via PbCl <sub>2</sub> .....	44
Table 5. PV parameters of the FACsPbI <sub>3</sub> via MAcl.....	44
Table 6. PV parameters of the FACsPbI <sub>3</sub> via FAcI.....	44
Table 7. PV parameters of the FACsPbI <sub>3</sub> via HCl.....	44

## ABSTRACT

In the recent years, the perovskite solar cells (PSCs) have evolved exponentially in terms of its efficiency since 2009 and since then there has been an enormous research in this field to pull up the efficiency. These accomplishments in the performance are by virtue of its superior optoelectronic properties that includes micrometre range diffusion lengths due to high crystallinity, strong light absorption potential with feasibility of band gap tuning, and ambipolar charge transfer capabilities. This project focused on two areas firstly on device fabrication along with its optimization and secondly to studying the effect of chlorine introduction in perovskite through various routes.

In the first half of the thesis, fabrication of the perovskite solar cells (MAPbI<sub>3</sub> and FACsPb(I<sub>0.83</sub>Br<sub>0.17</sub>)<sub>3</sub> based) were done along with the optimization in terms of temperature, RPM, spin coating time, annealing time and temperature followed by some characterisations. The other half was to studying the effect of chlorine introduction in perovskite through various routes. Different salts with significant stoichiometry were used to maintain the perovskite structure (ABX<sub>3</sub>). The chloride introduction was taken through organic salts as well as inorganic ones namely methyl ammonium chloride (MACl), formamidine hydrochloride (FACl), lead chloride (PbCl<sub>2</sub>) and hydrochloric acid (HCl). It was observed that the precursor which used Chloride through lead has a better optical properties in terms of defect states and charge transportation. Further the device fabrication were done by using these different perovskite precursor solution. Finally, it was found that the device in which chlorine is introduced from lead in the perovskite precursor has the highest efficiency among all.

# INTRODUCTION

When the global warming and depletion of common energy supplies, such as fossil fuels started out threatening to the balance of human life, notable interest was shown towards the renewable (alternative) energy sources. Among number of alternative sources, such as tidal energy, wind energy, geothermal energy and biomass, solar energy has the highest amount potentially available on earth. A very small fraction of sun power (less than 0.02 %) reaching the earth surface can cover the whole energy demand of the world.

There are various solar technologies for harvesting the sun energy, which can be divided to two categories: passive solar and active solar. An example of passive technique can be the designing of a building in such a way that it efficiently harvests and stores the sun energy in the building. Active solar technologies are the solar thermal collectors or photovoltaic (PV) devices. However, the fastest and most efficient direct conversion of sun light into electrical energy is possible only through PV devices. The photovoltaic effect discovered by Becquerel is the basic physical process, by which the semiconductor material converts electromagnetic radiation (sun light) into electric power [1].

The first generation conventional photovoltaic technologies have captured the marketplace due to their performance, long term stability and are playing a major role in the solar energy harvesting [2]. The challenge that Silicon photovoltaic industry faces today is that the cost of energy production is too high due to cost intensive processing techniques involved to achieve the purity of the material. While our surrounding is surrounded with huge amount of solar strength, the PV era continues to be too highly priced to grow to be a primary electricity source. Therefore, the main mission of the solar cell subject is to increase the technology, which could provide reasonably- priced PV merchandise and make the photo-conversion of suns light into electrical power cost efficient.

In the previous years, the photovoltaic studies has been evolved significantly; the important contribution imparted with the development of low value and highly efficient perovskite solar cell technology. The idea of perovskite devices was communicated by the Miyasaka's group in 2009 with the first ever perovskite based device with 3.9% power conversion efficiency [3]. After this breakthrough published, many research

groups took up the hot research area and the technology started to grow and achieved the efficiencies of 25.2% till the present [4].

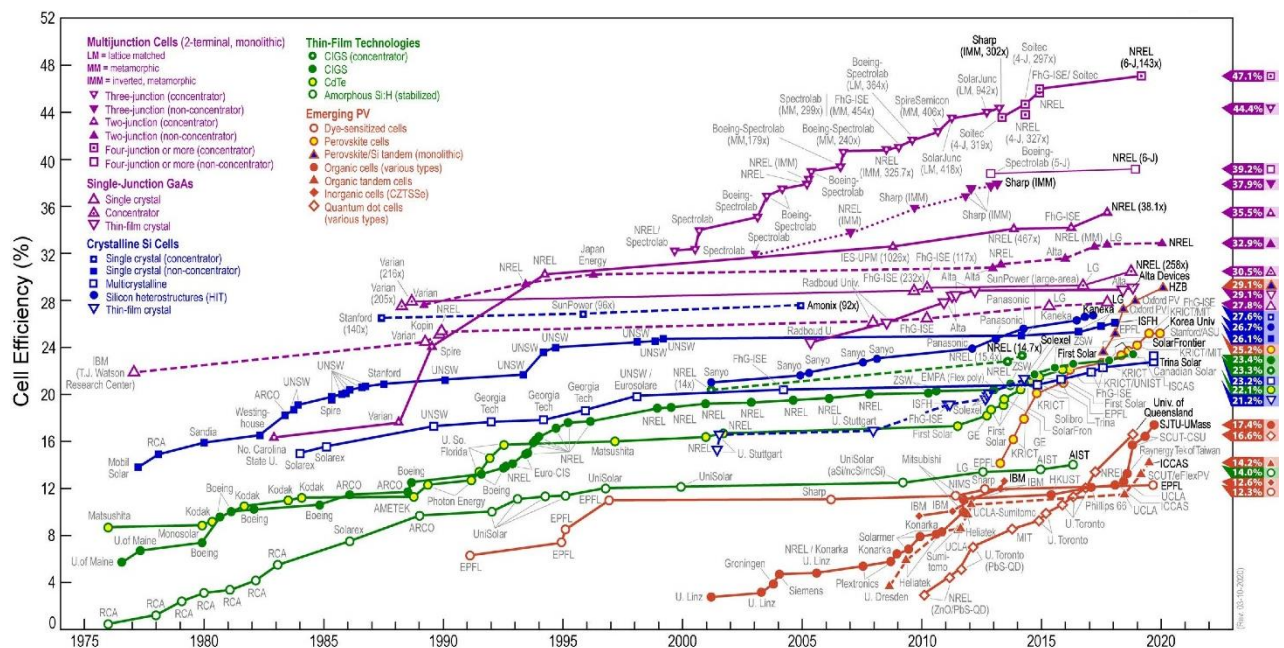


Figure 1. Cell efficiency chart [4]

The intense interest for this technology is attributed to its low fabrication cost and ease of synthesis that doesn't need any semiconductor device processing tools. These accomplishments in the performance is by virtue of its (a) superior optoelectronic properties that includes micrometre range diffusion lengths due to high crystallinity, strong light absorption potential with feasibility of band gap tuning, very low Urbach energy and ambipolar charge transfer capabilities (b) flexibility of tuning the optical, electrical and structural properties by compositional engineering of organic/inorganic part of the metal halide perovskite constituents [5]. Due to these exceptional properties and low cost fabrication methods, perovskite has even expanded its roots beyond the photovoltaic research that include light emitting diodes, memory storage devices and photo-detectors etc.

## 1.1: Solar Cell History

In 19<sup>th</sup> century, it was observed that the sunlight in terms of photon striking certain materials generates a detectable electric current which was referred to as the photoelectric effect. The history had laid the foundation of solar cells.

Researchers have classified solar cell generation based on the materials used, process involved, manufacturing system and the manufacturing cost of solar cells. Photovoltaic devices (solar cells) have so far been classified in three generations depending on the time period they started playing a vital role in the solar cell field [6]. The three generations of the solar cells are the first generation solar cells (1G), second generation solar cells (2G) and third generation solar cells (3G).

## 1.2: Generations of Solar Cells

1.2.1: First generation Solar Cells: 1G solar cells are based on mono crystalline and multi crystalline silicon. Crystalline silicon solar cells took their name from the manner they were made. The mono crystalline silicon solar cells were made from thin wafers that have been cut from a singular continuous crystal particularly grown for this purpose. Mono crystalline cells are darkish blue to black in colour (see figure 2) [7].

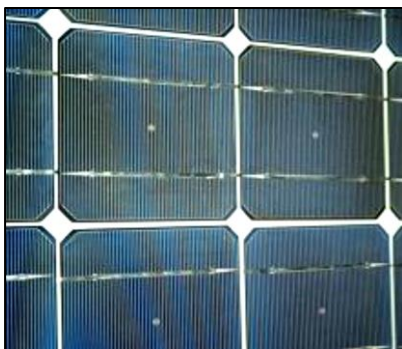


**Figure 2.** Monocrystalline Cell



**Figure 3.** Polycrystalline Cell

Poly crystalline silicon solar cells are made up by melting the silicon material and pouring it right into a mold. Since from the discovery at Bell Laboratories, the crystalline silicon solar cell performance has reached upto greater than 25% [8]. Polycrystalline cells also have a bluish colour but not as dark as mono crystalline cells. This cell type is made from polycrystalline silicon, which gives it the characteristic crystalline surface structure (see figure 3). This cell type is cheaper to manufacture compared to mono crystalline cells and the cell efficiencies are up to 20.4% [8].

The performance of pn-junction crystalline silicon solar cells could reach as much as the theoretically expected restriction of 30% [9]. In India, noteworthy work (studies) has been performed in this direction with polycrystalline silicon and monocrystalline silicon [10, 11]. Presently, silicon solar cells covers around 90% of the photovoltaic market because of their relatively high conversion performance, long term life stability and proven technology. The performance of commercial products in modules typically reaches near 15% to 20%. The manufacturing techniques which are being used to make first generation solar cells are very expensive, ensuing in years to pay again their shopping cost.

1.2.2: Second generation Solar Cells: In 2G solar cells, thin film technology or method has been used. These solar cells are thinner and flexible to some extent and less highly- priced compared to the 1G solar cells. Semiconductor materials for the 2G solar cells ranged from amorphous and micromorphous silicon [12, 13] to binary or quaternary semiconductors, such as cadmium telluride [14], gallium arsenide [15] and copper indium gallium selenide [16].

1.2.2.1: Amorphous silicon cells have a dark brown to purple colouring (see figure 4). The simplest cell structure consists of three layers (p-i-n). The production is cost effective but the cell efficiencies are only about 6-8% [13]. Stability and lifetime of such cells are the limiting factors of this technology.



**Figure 4.** Amorphous Silicon



**Figure 5.** Flexible CdTe Cells

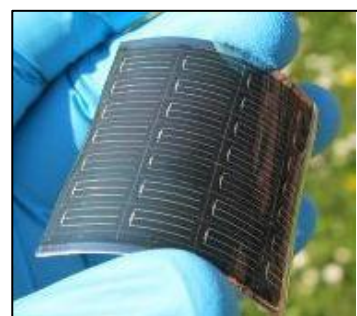


**Figure 6.** Flexible CIGS cells

1.2.2.2: Cadmium telluride (CdTe) cells, shown in figure 5, have efficiencies of about 17.3 % [14]. The limiting factor for these cells is the supply of the material Tellurium. Also the cadmium is extremely toxic and recycling of the old CdTe cells is an issue.

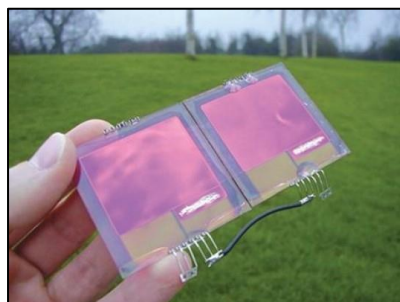
1.2.2.3: Copper indium gallium selenide solar cells shown in figure 6 has the maximum efficiency among the thin film cells with the power conversion efficiency (PSC) of around 20.3% [16]. Current disadvantages are the higher production costs compared to the other thin film technologies.

Other technologies of the second generation are multi-junction cells which contain many p-n junctions. The standard efficiencies for different multi-junction cells range from 32.6% to 43.5%. Specific p-n junctions are designed in multi junction cells to absorb the different wavelength of light and are positioned on the one another. This technique can be extended to silicon-crystalline cells and thin film cells with some restrictions on material choices. However, the multilayer cells production costs are very high and are used in more specialized applications such as the space industry or in desert areas with high concentration of sunlight.

Though the power conversion efficiency of these solar cells is lower than that of crystalline silicon solar cells, the 2G solar cells are expected to be price- effective in comparison to the value of energy production from the fossil fuels [8]. Unfortunately, there are nevertheless some unresolved troubles in commercializing these solar cells in terms of manufacturing at large scale portions at an aggressive cost (low cost) and at a reasonable performance level.

1.2.3: Third Generation Solar Cells: Organic solar cells (OSCs) and dye sensitized solar cells (DSSCs) are the cells with the most promise for devices of the 3rd generation. Organic molecules or conductive organic polymers (carbon-compound based) are used by OSCs as light-absorbing and charging fabrics, whereas DSCs use organic dyes to absorb photons. The benefits of the DSCs are that their efficiency increases with temperature, whereas the material and manufacturing costs on the other side are lower.

**Figure 7.** Organic Solar Cell



OSCs currently face problems due to degradation including low power conversion efficiencies and short lifespan. They have very low weight which makes them more cost efficient for applications where low weight is required. OSCs are durable, long-lasting and will not crack like traditional crystalline PV modules built on brittle glass substrates. However a big plus is that all OSC components are available and recyclable. Nevertheless, the hope is that solar cells of third generation will soon enter the market. The current level of OSC use is more focused on specific applications for example, clothing, pcs, smartphones or small portable devices [12].

1.2.4: Hybrid Solar Cells: In attention of the high performing and long term stability of inorganic solar cells and the relative low cost of the OSCs, the idea of fabricating more price- effective hybrid solar cells via combining organic materials and inorganic materials was brought in 2002 [17]. Semiconductor nanocrystals of lead sulphide, lead selenide, titanium dioxide, and zinc oxide have been used to make hybrid solar cells in aggregate without or with polymers.

So far hybrid cells are based upon organic compound such as Spiro-OMeTAD, FAI, MAI, etc along with the inorganic components such as lead  $PbCl_2$ , CsI, CsCl,  $PbI_2$ , etc [18]. Here, this project deals with the chlorine addition into the perovskite precursor by using both organic and inorganic salts ( $MACl$ ,  $FACl$ ,  $PbCl_2$  and  $HCl$ ) and the fabrication of perovskite solar cells.

### **1.3: What are Perovskites?**

The mineral (perovskite) was first discovered within the Ural Mountains of Russia and is later termed on the founder of Russian Geographical Society, Lev Perovski. The perovskite structure generally represents any compound that has the ditto structure as of the  $CaTiO_3$  mineral. The perovskite is shaped of titanium, calcium and oxygen in the form of  $CaTiO_3$ . Resembling the  $CaTiO_3$  structure, perovskites are the materials which are described by the formula  $ABX_3$ , where X is an anion and A and B are cations of different sizes (cation A being larger than cation B) [19]. The perovskite films can be processed using solution-based techniques like spin coating, spray coating, doctor blading, vapour deposition methods, etc.



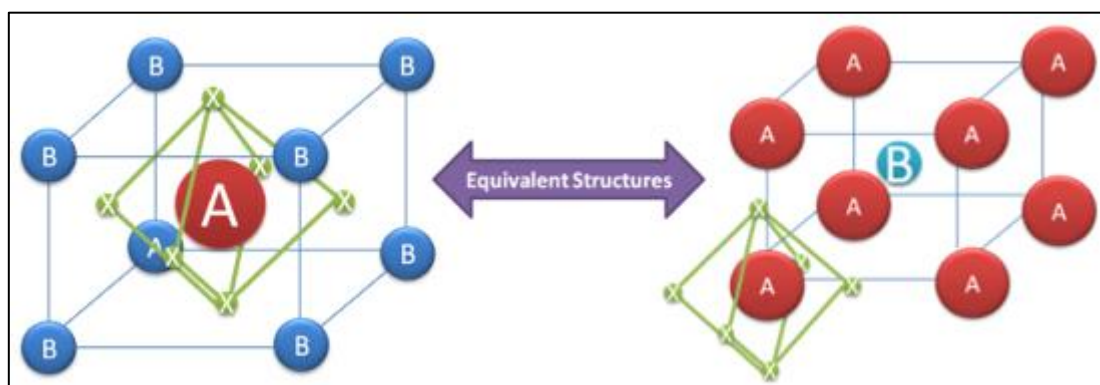


**Figure 8.** Perovskite crystal structure of the form  $ABX_3$

Depending on what atoms or molecules are being used within the perovskite structure, the perovskites can have quite excellent array of exciting properties, like giant magnetoresistance, superconductivity, spin-dependent transport (spintronic) and catalytic / optoelectronic properties. Therefore for physicists, chemists and material scientists, perovskites represent a playground.

The perovskites have been first utilized in solid-state solar cells in 2012 and since then the maximum cells have used following combination of materials within the usual perovskite structure  $ABX_3$  [20].

**A =** Organic cation- formamidinium ( $NH_2CHNH_2^+$ ) or methyl ammonium ( $CH_3NH_3^+$ )

**B =** Inorganic cation- generally lead ( $Pb^{2+}$ )

**X =** Halogen anion- usually chloride ( $Cl^-$ ) iodide ( $I^-$ ), bromide ( $Br^-$ ) or fluoride ( $F^-$ )

#### **1.4: Properties of Perovskite**

To understand the system degradation mechanism and carrier transport as well as to maximize the device efficiency we need to recognise the optical and electrical properties of the perovskite thin film. Listed below are the some properties of the perovskite which makes it significant.

1.4.1: Ambipolar Charge transport: Perovskite has a special characteristic property which shows the transportation of holes and electrons simultaneously.

1.4.2: Absorption coefficient ( $\alpha$ ): It is a very important property for the absorber layer. The more will be the absorption coefficient of the material, the thinner will be the

absorber layer (perovskite layer) which we want to effectively absorb the sun's incident light.

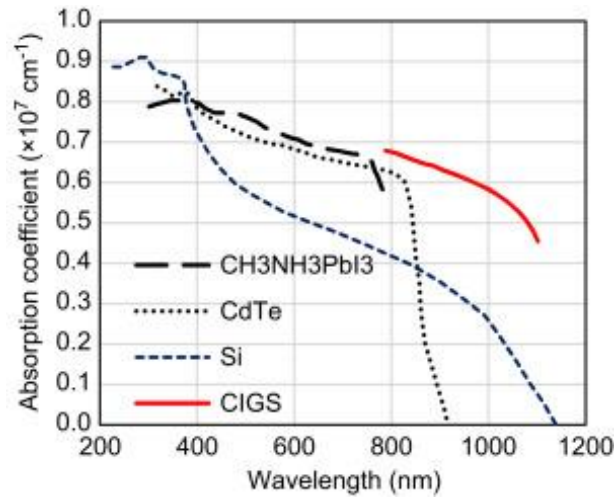


**Figure 9.** Absorption coefficient of PV materials

Figure 9, provides a comparison of the absorption coefficient between various photovoltaic materials at different wavelengths. This figure shows that perovskite has a significantly greater coefficient of absorption ( $\sim 10^5 - 10^6 \text{ cm}^{-1}$ ) relative to crystalline silicon [21]. It means that only about 100 nm- 1  $\mu\text{m}$  thickness of perovskite film is required to effectively absorb most of the sun's light.

**1.4.3: Bandgap ( $E_g$ ):** Bandgap is the most crucial parameter for a PV material. The maximum theoretical efficiency that can be gained depends on the material bandgap according to Shockley- Queisser limits. Perovskite is a material with direct bandgap. The bandgap of ant particular material can be found from  $\alpha^2$  vs  $h\nu$  "Tauc plot" [22]. The quantum efficiency is written as below,

$$QE(\lambda) = c\alpha(\lambda)t$$

Where, the thickness of the absorber film is  $t$ ,  $\alpha$  is the absorption coefficient at the incident wavelength  $\lambda$  and constant  $c$ .

The average efficiency which can be achieved by a single junction perovskite solar cell is nearly 31%, according to Shockley- Queisser limit [23]. The maximum efficiency for a double junction tandem solar cell and perovskite as a high bandgap material and either CIGS or c-Si as a low bandgap cell is nearly 44%. So, the perovskites could improve the power conversion efficiency enormously.

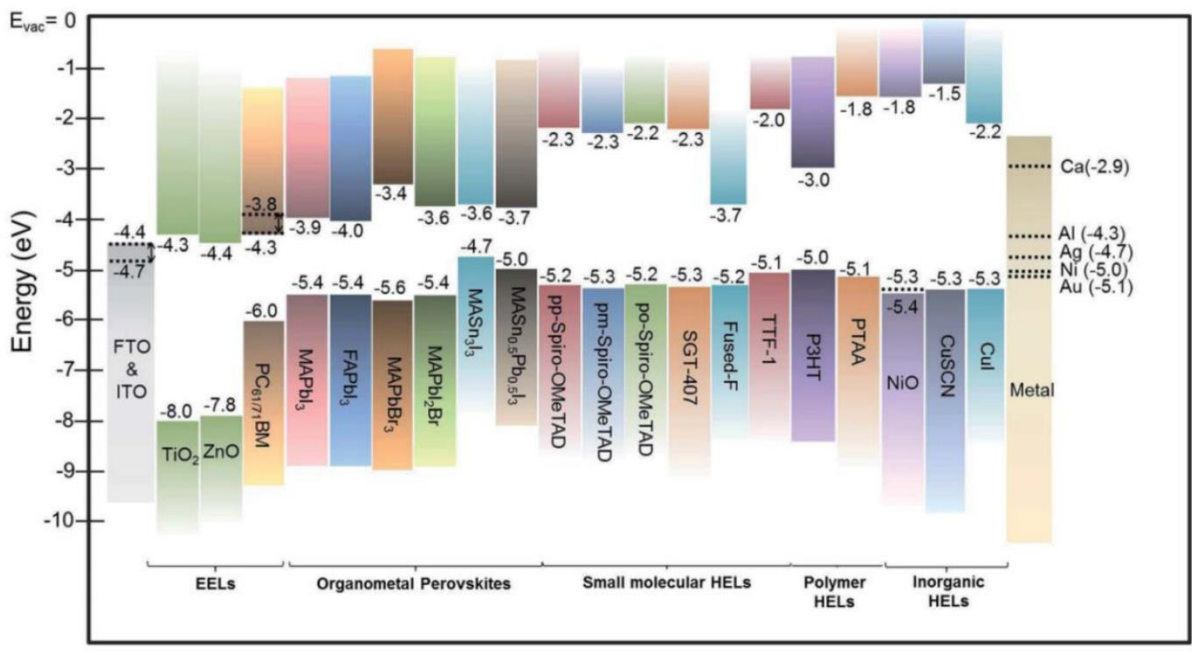


**Figure 10.** Energy bandgap of different materials

1.4.4: Diffusion length: The perovskites are also known to have a very high carrier diffusion length due to its higher crystallinity property. Some research groups have reported that the diffusion length is of the order of micro-meters [24, 25, 26]. La-ororakiat et al. used time resolved terahertz spectroscopy to measure the diffusion length of the carriers at different temperatures. They disclosed that the duration of the diffusion of electrons and holes can exceed upto 1  $\mu\text{m}$ . Diffusion lengths at normal room temp will differ from the other which is calculated at the low temperature, indicating the difference is the mechanism of recombination when temperature changes [26]. Several research groups [24, 25, 27] have reported that the perovskite have the very high carrier lifetime and carrier mobility, resulting in the long diffusion length and greater charge collection capacity.

# CHARACTERISATION TECHNIQUES

## 2.1: Photoluminescence spectroscopy (PL)

The study of the electromagnetic radiations with that of matter is known as spectroscopy. When a photon which is having an energy equal or greater than the band gap of material is absorbed, the electrons get excited from valance band to the conduction band and when the electrons relax through radiative recombination it emits a photon in the visible region without the generation of heat is photoluminescence.

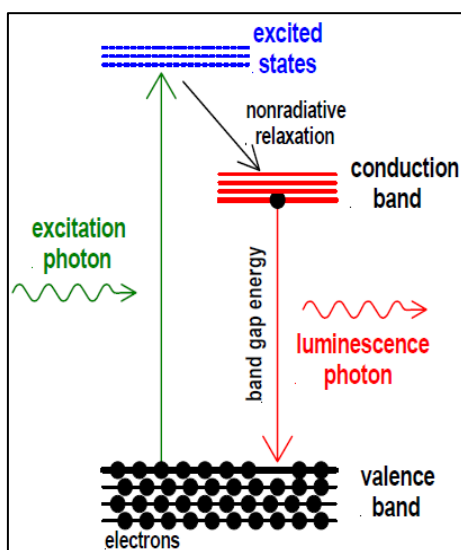


**Figure 11.** Principle of photoluminescence spectroscopy

All the PL measurements were done by SHIMADZU Spectrofluorometer RF-6000 having xenon arc lamp installed in it. This instrument is operated by LabSolutions RF software.



**Figure 12.** Instrumental setup of SHIMADZU RF- 6000PC Spectrofluorometer

## 2.2: Optical Microscope

Optical microscope is often known as the light microscope that uses one or a combination of lenses to magnify the sample images with the help of the visible light. The optical microscopy is a highly flexible imaging process used to determine the morphology of the top surface or crystal growth behaviour.

All the optical measurements were done by Olympus DP73- Advanced digital micro-imaging instrument.



**Figure 13.** Instrumental setup of Olympus DP73

## 2.3: X-ray Powder Diffraction (XRD)

XRD is an important tool which is used to determine grain size, lattice constants, solid solution composition and degree of crystallinity in the crystalline and amorphous material mixture [29]. This is a popular technique for studying crystal structures, atomic spacing, crystallite sizes, stress analysis, lattice parameters, quantitative phase analysis and it can provide details about unit cell measurements.

XRD evaluation is based totally on the constructive interference of monochromatic X-rays. The interplay of incident rays to the sample gives constructive interference and a diffracted ray when situation satisfies, the Bragg's Law equation

$$2 d \sin \theta = n \lambda$$

Here,  $n$  is number of refraction,  $d$  is distance between the planes and  $\theta$  is angle of diffraction. The stated law relates between the lattice spacing in a crystalline sample and the wavelength of electromagnetic radiation to the diffraction angle. It represents that the path travelled is same to the integral multiple of wavelength  $\lambda$ .

All the XRD measurements were done by RIKAGU SmartLab SE XRD machine.



**Figure 14.** Instrumental set up of XRD

#### 2.4: UV-Vis Spectroscopy

UV-Vis spectroscopy is used to determine the various amount of light which is absorbed, reflected or transmitted by the given sample, while deliberating the diverse phenomena capable of producing misleading measurements like diffusion, refraction and polarization. The spectral range that this tool occupies is from 175 nm to 3300 nm [30].

It measures the transmission or absorption in UV-Visible area. By absorbing the incident light, the molecule undergo an electrical transition from the ground state to

the one of discrete energy levels. Consequently, after passing the sample, the light got at the detector varies from the incident light in terms of intensity. Absorbance is normally given by;

$$A_{\lambda} = - \log \frac{I}{I_0}$$

where,  $A_{\lambda}$  is the absorbance at particular wavelength  $\lambda$ ,  $I$  is the intensity of light after passing through the sample and  $I_0$  is intensity of the incident light. Transmittance ( $I/I_0$ ) can be calculated from the absorbance equation.

The reflectivity measurements have been performed with Perkin Elmer Lambda 1050 UV/VIS spectrophotometer.



**Figure 15.** Instrumental setup of UV-Vis Spectrophotometer

## 2.5: Scanning electron microscopy (SEM)

SEM is used to produce images of the sample with help of scanning of the surface with the focused beam of electrons, mainly the back scattered electrons. It can achieve a resolution greater than 1 nm. It includes the surface analysis like the surface morphology, roughness, cracks etc.

The presence of EDX capability with SEM instrument is very beneficial for quantitative and qualitative analysis for any specimen. EDX is an analytical tool used to analyse a sample elementally or to classify it chemically. This is based on sample study of interactions between matter and electromagnetic radiation, a study of X- rays emitted by matter in response to the electromagnetic radiation being struck. Characterization capabilities are largely due to the fundamental idea that each element has a unique

atomic structure that enables X-rays characteristic of atomic structure of an element to be differentiated from each other in a specific way [31].

## 2.6: I-V measurement (Solar cell testing)

The solar simulator is a source of light with a wide band optical output close to the sun in the response range of different solar cell technologies. Solar simulators are being used for electrical analysis of solar devices. The I-V characteristics have been measured using the Oriel Sol3A Solar Simulator (94123A) attached along with Keithley 2440 5A SourceMeter. This is the most significant and fundamental characterization of any solar cells. Xenon arc lamp is used to illuminate solar cells of size at intensity set to 1 sun. The xenon simulator provides a reasonably good match for the spectrum of the sun.

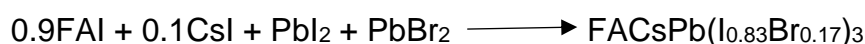
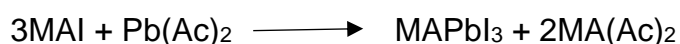


**Figure 16.** Instrumental setup of I-V Measurement



## Device Fabrication

The study of the any perovskite material is incomplete with a device fabrication. Initially I have fabricated the devices of MAPbI<sub>3</sub> (via acetate route) and FACsPb(I<sub>0.83</sub>Br<sub>0.17</sub>)<sub>3</sub>, simultaneously by optimizing the different layers used in the device i.e., ETL, active layer and HTL. The chemical equation which are considered during the perovskite synthesis are listed below.



### **3.1 Device physics of solar cells**

Solar cell which is also known as photovoltaic device is an electrical cell which converts the light energy into the electrical energy by the process known as photovoltaic effect. The sources of light can be sunlight or an artificial light. This electrical device uses the renewable source of energy to provide electricity which is one of the primary needs of mankind. As the word 'electricity' suggests, it's the play of 'electrons'. Photovoltaic effect is based on absorption of photons and generation of electron and hole pairs which are separated and connected to an external circuit. This method induces a material that can absorb light in order to generate electron and hole pairs. The electron and hole pair produced can be diffused and drifted until the contact layers are collected. Higher energy electrons and holes will flow through the solar cell's external circuit and produce photo-current. At the end of the day, those high energy holes and electrons emit energy to an external load circuit then return to the device and then recombines. Other than charge generation or transport, the recombination of the charge carriers and ion migration are the basic physical processes that govern the operation of perovskite solar cells. To maximize the stability and efficiency of PSCs, understanding the interplay between these physical processes is essential.

Below are the four processes that plays the role in photovoltaic energy production:

- absorption of incident photons
- generation of free electron and hole pairs
- transportation of photo generated charge carriers
- collection of photo generated charge carriers

In perovskite solar cells, there are five layers namely bottom electrode (counter electrode / cathode), electron transport layer (ETL), perovskite film (active layer), hole transport layer (HTL) and top electrode (anode). The basis for selecting each layer depends on the energy level. Electrons flow towards lower energy levels of conduction band while holes flow to the higher energy level of valence band. So with respect to perovskite, the ETL should be at a lower energy level and the HTL should be at a higher energy level. Electrons flow from anode to cathode and the current flow in the opposite direction.

The configuration of the sandwich style system can aid in the efficient carrier collection. The sandwich type of structure is divided into two different types: (i) pin and (ii) nip. If the sunlight occurs first on the p layer (hole transport layer / anode) followed by the absorber i-layer (electron transport layer) and n layer (cathode), then this solar cell architecture is called as pin structure. And If the sunlight enters the device through n layer (electron transport layer / cathode) before getting absorbed in the absorber i-layer (hole transport layer) followed by p layer (anode), then this solar cell architecture is referred as nip structure. There are different choices for each of these layers based upon their properties and requirements.

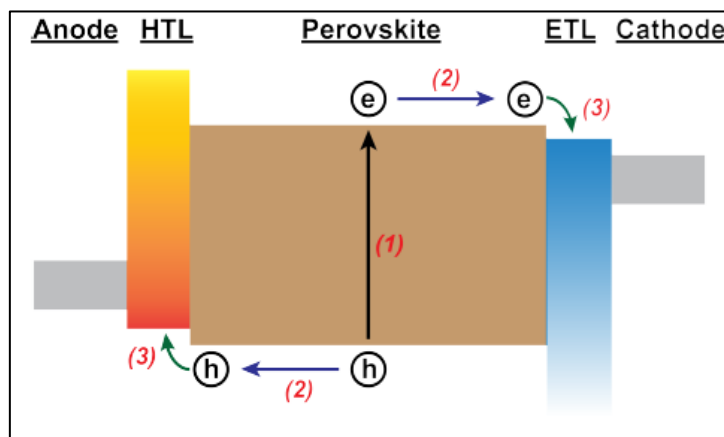


**Figure 17.** The schematic sketch of a perovskite solar cell and its working

Step (1): Generation of free holes & electrons upon light absorption by the perovskite

Step (2): Transport of charge carriers by drift and diffusion phenomena

Step (3): Charge carrier transfer to respective transport layers and eventual extraction at the electrodes

## 3.2: Methods and Experimental Details

3.2.1: Chemical used: Methyl ammonium iodide (MAI) was purchased from GreatCell solar. Lead acetate trihydrate ( $\text{Pb}(\text{CH}_3\text{COO})_2 \cdot 3\text{H}_2\text{O}$ ) was purchased from Sigma Aldrich, FAI, CsI,  $\text{PbI}_2$  and  $\text{PbBr}_2$  were bought from TCI. Spiro- OMeTAD was purchased from Luminescence Tech. Corporation, HCl was purchased by Loba Chemicals. Gold and silver for electrodes were purchased from sigma. Other chemical solvents or chemicals including N, N- dimethylformamide, acetone, isopropanol, etc. were purchased from Sigma- Aldrich. All the chemicals were used as received.

3.2.2: Synthesis of Electron Transport Layer: c-TiO<sub>2</sub> (compact-titanium dioxide) films are generally used as an electron transport layer (ETL) in perovskite solar cells, which is only electron selective layer and helps the cell to extract electrons from the perovskite light absorbing layer and then transport them to electrodes [32]. It is the thickness of c-TiO<sub>2</sub> that plays crucial role in extracting the electrons from perovskite film. Ideal thickness of c-TiO<sub>2</sub> should lie between 50-90 nm. So, we have optimised the thickness of c-TiO<sub>2</sub> by varying the speed and time of spin coating and the thermal annealing time of the films fabricated.

TiO<sub>2</sub> was prepared by sol-gel method which is given in the reference [33]. TiO<sub>2</sub> was deposited onto clean glass substrates. The substrate were cleaned by the standard protocol sequentially in soap water, deionised water, acetone and IPA in sonication bath for ten minutes followed by plasma cleaning [34]. The plasma cleaned substrates were used for TiO<sub>2</sub> coating at 2000 rpm for 45 seconds under ambient conditions (RH=65%). The step-by-step sintering of the thin films set at 100°C, 200°C, 300°C, and 500°C for 10 minutes, 20 minutes, 30 minutes and 2.5 hours respectively on a ramped hot plate.

3.2.3: Synthesis of Perovskite film: The perovskite material used is 30wt% Methyl ammonium lead triiodide ( $\text{MAPbI}_3$ ) synthesized by mixing lead acetate trihydrate, MAI in solvent DMF [35]. The precursor was then heated for 30 minutes at 50°C and spin coated onto the glass substrate using single step process at 2000 rpm for 30 seconds under ambient conditions (RH=65%). Then, the film was annealed at 150°C for 1 hour.

On the other hand, 1.45 M of  $\text{FACsPb}(\text{I}_{0.83}\text{Br}_{0.17})_3$  perovskite solution is prepared using FAI, CsI,  $\text{PbI}_2$  and  $\text{PbBr}_2$  in DMF: DMSO (4:1) as a solvent. The precursor was spin coated on the glass substrate using single step process at 6000 rpm for 35 seconds

under ambient conditions (RH= 30%). Then, the perovskite film was also annealed at 100 °C for 30 minutes in ambient conditions (30% RH).

3.2.4: Synthesis of hole transport layer: The 10wt% Spiro- OMeTAD in chlorobenzene has been used as a hole transporting material. This layer is holes selective and initiates the hole transport toward the electrode meanwhile repelling the electrons towards the opposite direction i.e., ETL. It is hydrophobic in nature hence prevents the attack of moisture in the perovskite to some extent. The Spiro- OMeTAD solution was doped with 20 $\mu$ L lithium- bis (trifluoromethanesulfonyl) imide (LiTFSI) and 4.8 $\mu$ L 4-tert-butylpyridine (t-BP) to increase the holes mobility [36].

3.2.5: Device fabrication: The fabrication of perovskite solar cells were done on fluorine-doped tin oxide (FTO) - coated glass substrates which has the resistance of approximately 7  $\Omega$  cm<sup>-2</sup>. The FTO glass substrates were patterned and etched with Zn-power and 2M aqueous HCl (37%) followed by cleaning sequentially in soap water, deionized water, acetone, and IPA. After oxygen plasma treatment (which removes organic components) from FTO surface, a compact TiO<sub>2</sub> layer (electron transport layer) was deposited by spin coating. The step-by-step sintering of the thin films were done at 100°C, 200°C, 300°C, and 500°C for 10 minutes, 15 minutes, 15 minutes and 30 minutes respectively on a ramped hot plate. The MAPbI<sub>3</sub> and FACsPb(I<sub>0.83</sub>Br<sub>0.17</sub>)<sub>3</sub> perovskite films were deposited on c-TiO<sub>2</sub> coated FTO by spin-coating technique. During spin coating, anisole (50  $\mu$ L) was dripped on the FACsPb(I<sub>0.83</sub>Br<sub>0.17</sub>)<sub>3</sub>. The MAPbI<sub>3</sub> coated substrates were dried for 5 min at room temperature followed by annealing at 100°C for 10 minutes. FACsPb(I<sub>0.83</sub>Br<sub>0.17</sub>)<sub>3</sub> coated substrate were annealed at 100°C for 15 minutes. The 10wt% Spiro- OMeTAD in chlorobenzene doped with LiTFSI, hole transport material layer was then deposited by spin coating on the top of the perovskite coated FTO substrates. The devices were then kept in a desiccator for ~20 hours having oxygen rich environment. Lastly, a 150 nm thick silver contacts which served as the top electrode were deposited through a shadow mask by vacuum thermal vapour deposition technique (10<sup>-7</sup> Torr at rate of 0.2 nm/s) with an active area of 0.1 cm<sup>2</sup>.

## Steps involved in perovskite device fabrication

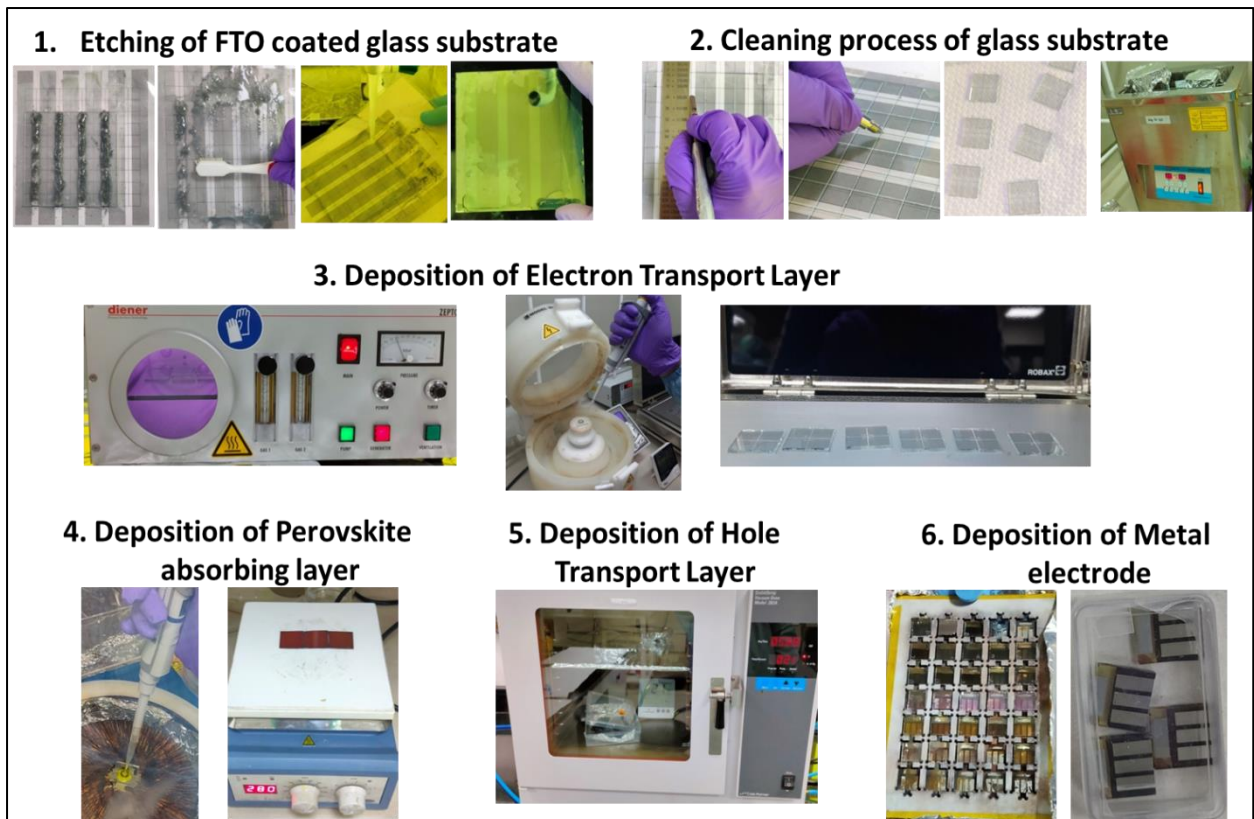


**Figure 18.** Steps involved in perovskite device fabrication

**3.2.6: I-V Characterisation:** Lastly the I-V characteristics have been done using the Oriel Sol3A Solar Simulator (94123A) attached along with Keithley 2440 5A SourceMeter. This is the most important and fundamental characterisation of solar cells which tells about the device efficiency. Xenon arc lamp is used to illuminate the solar cells at intensity set to 1 sun.

**Theory of I-V Characteristics:** The I-V curve is an exponential representation of voltage applied and the current flowing through the device under both light and dark conditions. The shape and details of curve can itself provides major properties of the electronic devices. The I-V equation of a solar cell can be derived in similar way as it has been derived for a P-N junction diode. When there is no light present to produce any current, the PV cell behaves sort of a diode and as the incident light intensity increases, then the cell generates current as shown in the figure 19.

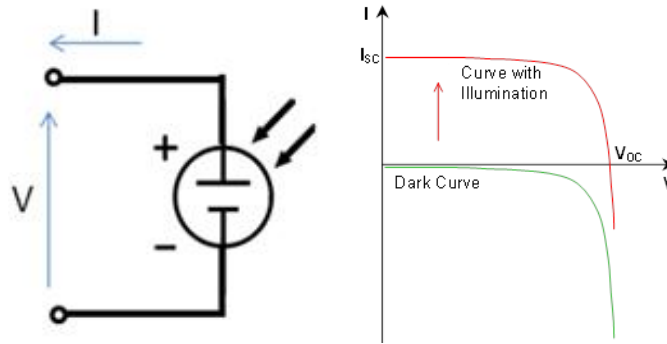


**Figure 19.** Shifting of I-V curve

There are four basic parameters of a solar cells on the basis of which they are compared with each other: efficiency ( $\eta$ ), Fill factor ( $FF$ ), open circuit voltage ( $V_{oc}$ ) and short circuit current ( $I_{sc}$ ). These parameters can be represented using figure 20.

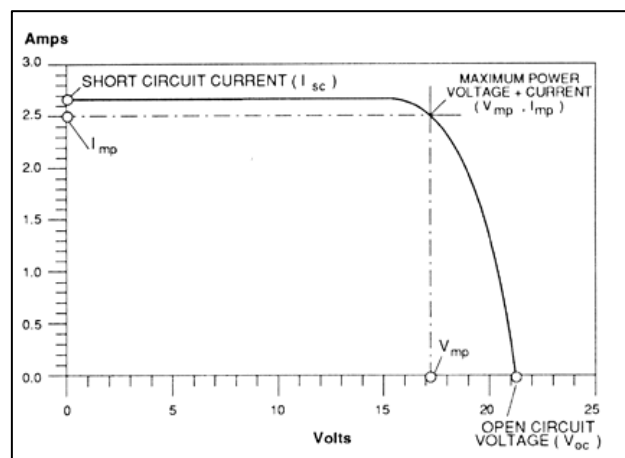


**Figure 20.** Solar cell I-V curve and its parameters

**3.2.6.1: Short circuit current ( $I_{sc}$ ):** It is the highest current which flows in a solar device when the terminal is on the P- side and the N- side are shortened i.e.,  $V = 0$  (figure 20). The short circuit current is nothing but a light-generated current. The short-circuit current is thus the maximum current from the solar cell that can be drawn. The short-circuit current density is used to estimate the  $I_{sc}$ 's reliance on the solar cell area;  $J_{sc}$  is also used to define the maximum current a solar cell is delivering. The overall current the solar cell is able to generate strongly depends on the solar cells optical properties like absorption in the absorber layer and the absolute reflection of the device. It is represented by current density and current per unit area, by the  $\text{mA}/\text{cm}^2$ .

**3.2.6.2: Open circuit voltage ( $V_{oc}$ ):** As the name implies, it is the maximum voltage generated across the terminal of a solar cell when they are kept open i.e.,  $I = 0$  (figure. 20). The  $V_{oc}$  depends on the light generated current and reverse saturation current. Generally the  $V_{oc}$  is given in by of mv or V. With increase the  $V_{oc}$  of the cells the

efficiency of the cell also increases. Practically for perovskite solar cells max 1.31 eV can be obtained.  $V_{oc}$  depends on the photo generated current density [38].

$$V_{oc} = \frac{kT}{q} \ln \left( \frac{J_{ph}}{J_o} + 1 \right)$$

3.2.6.3: Fill factor (FF): It represents the square ness of the I-V curve. Greater the square ness better is the properties. Also it shows the deviation of the curve from the ideal curve. Here the resistive losses both series resistance and shunt resistance are taken under consideration. The deal fill factor should be 1 or 100%, practically we obtain a max of 83%.

It can also be said as the ratio of maximum power ( $P_{max}$ ) =  $V_m J_m$  that can be extracted from a solar cell to the ideal power ( $P_o$ ) =  $V_{oc} J_{sc}$ . [39].

$$FF (\%) = \frac{V_m J_m}{V_{oc} J_{sc}}$$

3.2.6.4: Efficiency ( $\eta$ ): It is also called the power conversion efficiency or PCE. It can be stated as the ratio of the output power derive / extracted from the solar cell to the power input ( $p_{in}$ ) which is 1000 W/m<sup>2</sup>. The maximum power point ( $p_m$ ) of a solar cell is called the power output. Certainly the efficiency is dependent upon the temperature. We can say that with increase in temperature the efficiency decreases. Hence a solar cell works better in a low temperature.

$$\eta = \frac{V_m J_m}{P_{in}} = \frac{V_{oc} J_{sc} FF}{P_{in}}$$

The  $\eta$  shows that how much efficient the solar cell is.

### 3.3: RESULT AND DISCUSSION:

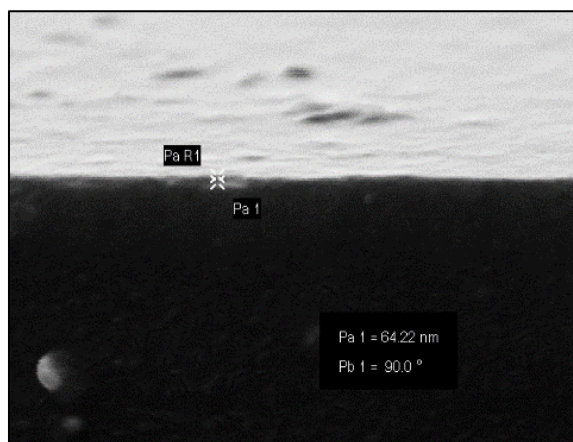


**Figure 21.** SEM image of c-TiO<sub>2</sub>

It is reported that 50-80 nm of c-TiO<sub>2</sub> layer thickness results in better charge collection and transfer. With prior optimisation of the c-TiO<sub>2</sub> thickness was reduced from 1.1 μm to 64 nm which initiates a better charge transfer or better transfer of electrons to the electrodes. The TiO<sub>2</sub> thickness was confirmed through the cross-sectional SEM image (figure. 21)

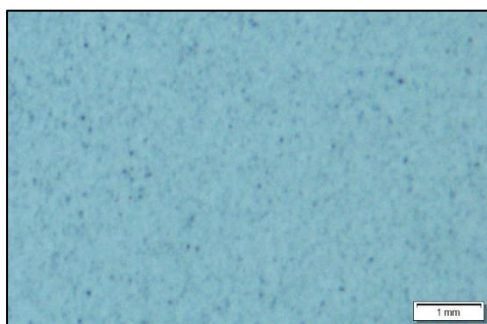


**Figure 22.** Optical of MAPbI<sub>3</sub>



**Figure 23.** Optical of FACsPb(I<sub>0.83</sub>Br<sub>0.17</sub>)<sub>3</sub>

The figure. 22 and figure. 23 above shows the optical images of MAPbI<sub>3</sub> and FACsPb(I<sub>0.83</sub>Br<sub>0.17</sub>)<sub>3</sub> perovskite films. The figure. 22 shows us the presence of pinholes that can act as short circuit. Figure 23 has a well-defined coverage with smaller grain size. We can see that the grain size in both the MAPbI<sub>3</sub> and FACsPb(I<sub>0.83</sub>Br<sub>0.17</sub>)<sub>3</sub> perovskite films are very small and cannot be seen through optical microscope. So, the SEM was performed to examine the morphology of the top surface.



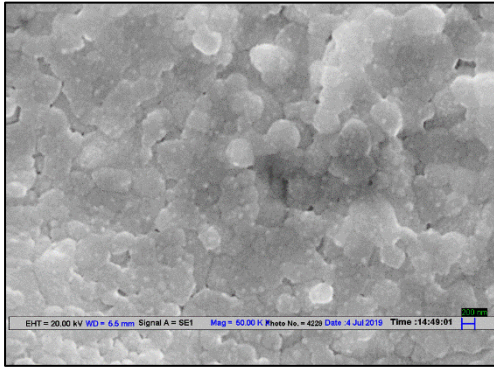


**Figure 24.** SEM of MAPbI<sub>3</sub>

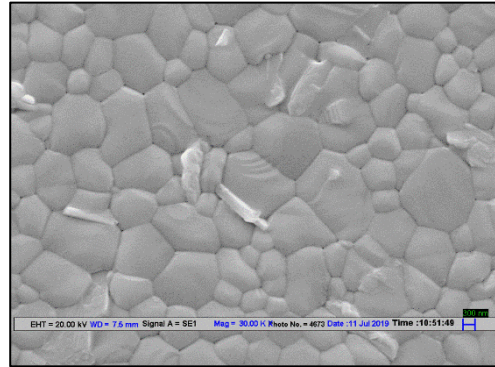


**Figure 25.** SEM of FACsPb(I<sub>0.83</sub>Br<sub>0.17</sub>)<sub>3</sub>

We have used SEM data to study the morphology of the top surface. Figure. 24 and 25, represents the morphology of the top surfaces of MAPbI<sub>3</sub> and FACsPb(I<sub>0.83</sub>Br<sub>0.17</sub>)<sub>3</sub> perovskite films. It is clearly seen in the images that the FACsPb(I<sub>0.83</sub>Br<sub>0.17</sub>)<sub>3</sub> perovskite film shows full coverage and ordered grains with no pin holes and grains having size ~100nm as compared to MAPbI<sub>3</sub> perovskite films.

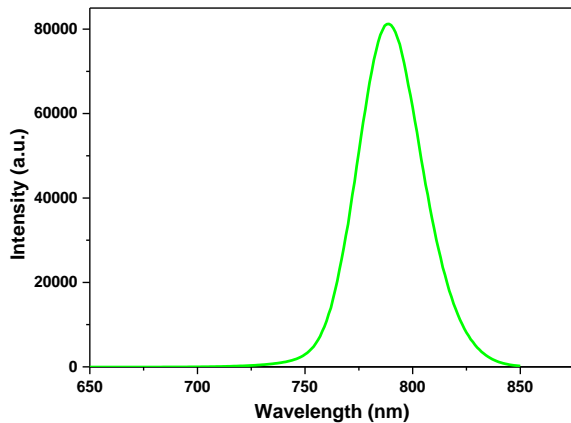


**Figure 26.** PL of MAPbI<sub>3</sub>

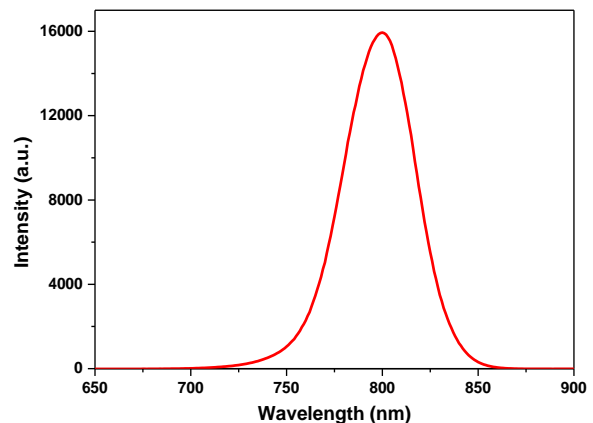


**Figure 27.** PL of FACsPb(I<sub>0.83</sub>Br<sub>0.17</sub>)<sub>3</sub>

Figure 26 and 27 drives the Photoluminescence Intensity of MAPbI<sub>3</sub> and FACsPb(I<sub>0.83</sub>Br<sub>0.17</sub>)<sub>3</sub> based perovskite films respectively. The Photoluminescence graph depicts the radiative and non-radiative recombination. Perovskite being a direct band- gap material with the bandgap of 1.55 eV favours radiative recombination. From this we can draw an information that the trap/ defect states are responsible for the loss of electron are less. The MAPbI<sub>3</sub> film has the maximum peak at 780 nm with the intensity of 80,000 and FACsPb(I<sub>0.83</sub>Br<sub>0.17</sub>)<sub>3</sub> film has the maximum peak at 800 nm with the intensity of 16,000.

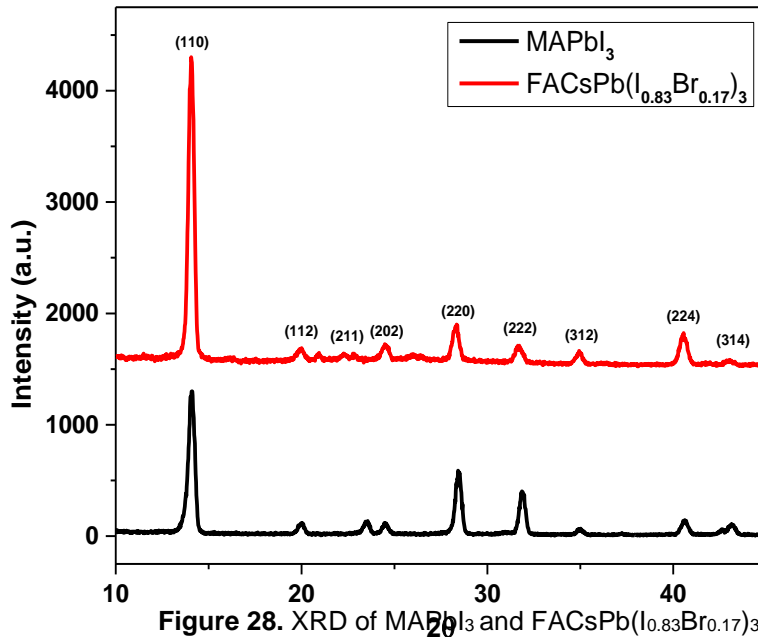


Figure 28. XRD of MAPbI<sub>3</sub> and FACsPb(I<sub>0.83</sub>Br<sub>0.17</sub>)<sub>3</sub>

The prominent peaks at 14.8°, 28° represents that the complete perovskite phase is formed with no traces of PbI<sub>2</sub> left (figure 26). This can be predicted by a missing peak at 12° which represents the formation of PbI<sub>2</sub>. The crystal structure of perovskite films which is measured by XRD depicts sharp and high intense peaks showing a highly crystalline nature of the perovskite films. The plane of diffraction corresponding to the 2 theta value are also indicated above. The highest peak stands at (110) plane having the highest intensity of approximately 3000 a.u. for FACsPb(I<sub>0.83</sub>Br<sub>0.17</sub>)<sub>3</sub> and an intensity of 1200 a.u. for MAPbI<sub>3</sub> films.

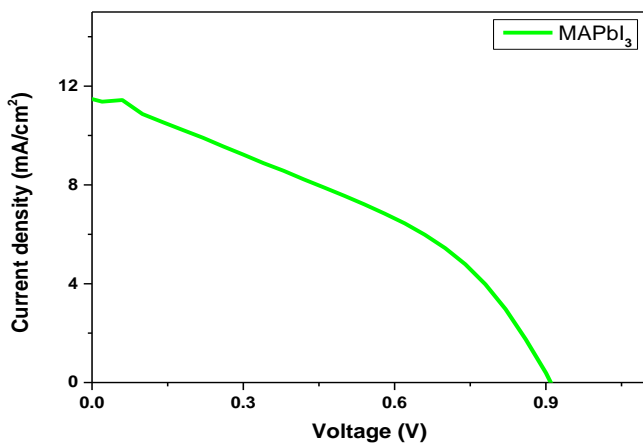


Figure 29. J-V curve of MAPbI<sub>3</sub>

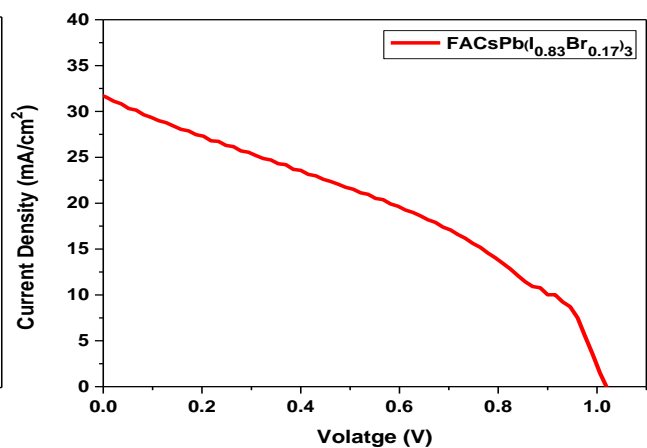


Figure 30. J-V curve of FACsPb(I<sub>0.83</sub>Br<sub>0.17</sub>)<sub>3</sub>

<b>Voc (V)</b>	0.9
<b>Jsc (mA/cm<sup>2</sup>)</b>	11.48
<b>Fill Factor (%)</b>	38.3
<b>Efficiency</b>	5.24%

**Table 1.** PV parameters of the MAPbI<sub>3</sub>

<b>Voc (V)</b>	1.01
<b>Jsc (mA/cm<sup>2</sup>)</b>	31.8
<b>Fill Factor (%)</b>	37.4
<b>Efficiency</b>	12.0%

**Table 2.** PV parameters of FACsPb(I<sub>0.83</sub>Br<sub>0.17</sub>)<sub>3</sub>

The Figure 29 and 30 represents the J-V curve of the c- TiO<sub>2</sub> / MAPbI<sub>3</sub> / Spiro-OMeTAD and c- TiO<sub>2</sub> / FACsPb(I<sub>0.83</sub>Br<sub>0.17</sub>)<sub>3</sub> / Spiro- OMeTAD based perovskite devices under illumination. Previously the device fabricated by MAPbI<sub>3</sub> based perovskite recorded an efficiency of 3.7%. With continuous trail and optimisation we achieved an efficiency of 5.24% for MAPbI<sub>3</sub> and another device of FACsPb(I<sub>0.83</sub>Br<sub>0.17</sub>)<sub>3</sub> based perovskite being 12% efficient. Table 1 and 2 shows the photovoltaic parameters of the MAPbI<sub>3</sub> and FACsPb(I<sub>0.83</sub>Br<sub>0.17</sub>)<sub>3</sub> based perovskite devices. We know that the maximum theoretical fill factor ranges from 83-85%, but in the above J-V curves we noticed a fill factor of 38.3% and 37.4%. Both the graphs indicates the presence of shunt resistance due to which there is a loss in the fill factor.

# Studying the Effect of Chlorine Introduction in Perovskite through Various Routes

It has been earlier reported in the literature that the presence of chloride in the perovskite precursor helps to improve the optoelectronic properties of the material. It plays a vital role from where the chloride is coming from. It was also clear that chlorine will not stay in the lattice but will help in the defect passivation of the perovskite film. Hence we have experimented to form the precursors through 4 different salt addition namely MACl, FACl, HCl, PbCl<sub>2</sub>.



## **4.1: Methods and Experimental Details:**

4.1.1: Chemicals used: Methyl ammonium Iodide (MAI) and Formamidinium Iodide (FAI) were purchased from TCI. Hydrochloric acid (HCl) was purchased from Loba Chemicals, Lead Chloride (PbCl<sub>2</sub>) from Sigma Aldrich, Caesium Iodide from TCI. Other solvents or chemicals including DMF, Acetone, IPA etc. were purchased from Sigma-Aldrich. All the chemicals were used as received. MACl and FACl were synthesized in the laboratory.

4.1.2: MACl and FACl Synthesis: For the preparation of MACl – 100ml ethanol was mixed with 24ml Methyl amine. This solution was taken in a flask placed upon a stirrer along with ice bath which was filled with ice. Now 10ml of HCl was added drop by drop along with stirring. Then the reaction mixture was put on stirring for half an hour. Then it was poured into a cleaned petri dish and covered with foil having holes and left for overnight. The next morning the salt left was scratched and collected and then washed with di ethyl ether for removing the impurities (done 3 times for half an hour each). After washing ethanol was added and it was left to recrystallize in the refrigerator overnight. Lastly, ethanol was removed and crystals formed were poured into the petri for oven heating at 60°C to obtain MACl.

FACl was also prepared in the similar fashion by mixing 10.41mg of Formamidinium Acetate with 6.145 millilitres of Hydrochloric acid.

4.1.3: Perovskite Precursor Preparation: For the precursor (A, B, C) firstly FAI & PbI<sub>2</sub> was dissolved in DMF: DMSO (4:1) and then CsI was Added followed by HCl, MACl & FACl respectively. While for precursor (D) FAI & MAI were dissolved in DMF: DMSO (1:4) followed by addition of PbCl<sub>2</sub> and lastly CsI was added and heated overnight at 70°C.

4.1.4: Synthesis of Perovskite film: The substrate were cleaned by the standard protocol sequentially in soap water, deionized water, acetone and IPA in ultra-sonication bath for 15 minutes followed by oxygen plasma cleaning [40]. Films were coated by spin coating method. 100µl of the individual precursor was spin coated onto plasma cleaned glass substrates. The films were coated at 1500 rpm for 45 seconds and heated at 150°C under ambient conditions.

Now preceding with the project, following are the experiments that were carried out:

- 1) The perovskite coated films were annealed at 150°C for 45 minutes at different humidity's - (10%, 20%, 30%, 40% and 50%) in Dry air (Oxygen) controlled environment to check the best humidity range for film fabrication. We concluded that a better film were obtained for 30% humidity in O<sub>2</sub> environment.
- 2) Further keeping 30% humidity as a reference we have optimised the perovskite films. The 1 M solution of the above mentioned perovskite precursor have been prepared and the films were optimised at different RPM of spin coating, spin coating time and annealing time as well as annealing temperature of the perovskite film.
- 3) Finally, the devices of all 4 precursors were fabricated by on FTO glass substrate. The gold as a top counter electrodes was deposited by thermal vapour deposition system and the IV measurement were carried out to measure the device efficiency.

## 4.2: RESULT AND DISCUSSION:

**4.2.1:** Firstly, the perovskite films were coated by spin coating technique. 100  $\mu\text{l}$  of individual precursor was taken and spin coated at 2000 RPM with 500 acceleration for 45 seconds. The coated films were then annealed under different controlled humidity ranging from 10-50% under  $\text{O}_2$  environment at 150  $^\circ\text{C}$  for 40 minutes.

After the film formation the morphology, photoluminescence intensity of the films were checked by using the optical microscope and photoluminescence spectrometer respectively. The respective data are compiled below:

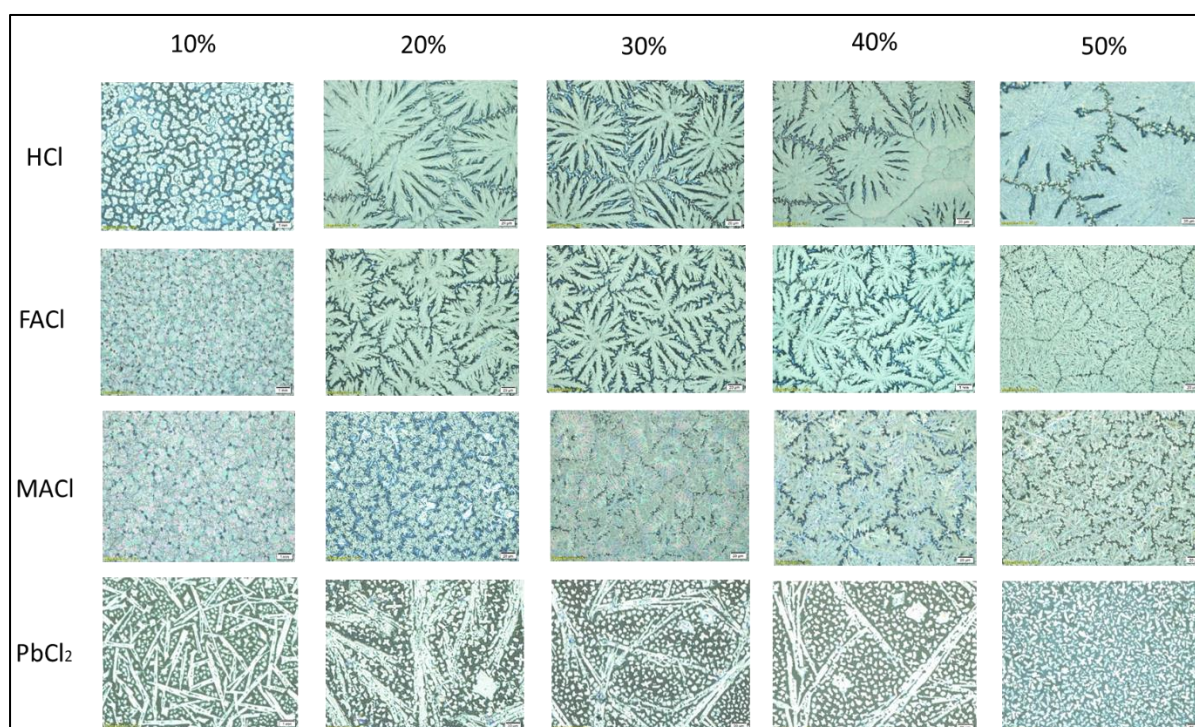


**Figure 31.** Comparison of optical images in different humidity in  $\text{O}_2$  environment

Figure 31, above deals with the optical images of perovskite films through HCl, FAcI, MACl and  $\text{PbCl}_2$  fabricated under an ambient condition and annealed under controlled humidity (10% , 20% , 30% , 40% and 50%) respectively. For HCl films under 10% had a very small grain size , which increased at 20% and they had the biggest grain size with better coverage under 50%. In case of FAcI , 10% humidity a proper coverage was seen but with a very small grain size. A similar morphology was observed under 20% , 30% and 40% but a better structure was concluded to be at 50% humidity.  $\text{PbCl}_2$  as seen in the figure 1. had rod like structures which decreases as the humidity increases.

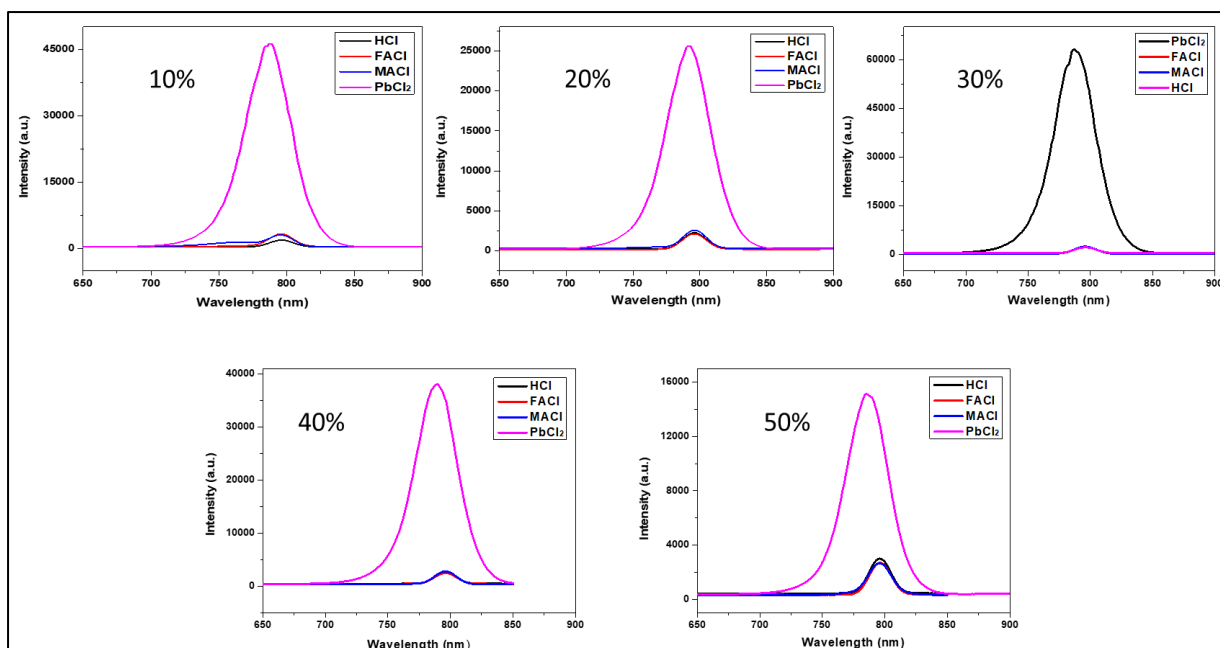


**Figure 32.** Comparison of PL in different humidity in O<sub>2</sub> environment

Figure 32, shows the Photoluminescence intensity data of perovskite film at different humidity levels (10% , 20% , 30% , 40% and 50%). We observe the films with HCl, FAcI and MACl had a lower count ranging from 4000 to 6000 a.u. in the humidity conditions. While on the other hand film with PbCl<sub>2</sub> shows a significant PL count of 46000, 27000, 65000, 35700 and 15000 a.u. at 10% , 20% , 30% , 40% and 50% relative humidity respectively.

Hence, from the morphology of perovskite films we observe that the PbCl<sub>2</sub> film did not have a good morphology as it has very small grain size which shows that the crystallisation is poor yet in the PL intensity data there is a significant highest PL intensity for PbCl<sub>2</sub> film at 30% RH in oxygen environment. Therefore despite of having a poor coverage in the PbCl<sub>2</sub> films at 30% RH, we obtained very high count intensity in PL. So 30% RH has been taken as a standard humidity for all the perovskite film formation in the upcoming experiments.

**4.2.2:** Now, the experiments were performed for 30% RH by the optimization of the films in terms of spin coating time, RPM, acceleration, annealing time and temperature of the perovskite films. We played with the different variables like the RPM of spin coating, spin coating time and annealing time as well as annealing temperature of the perovskite film. And the standard parameters for this experiments decided on the basis of the above mentioned variables were taken as 100 µl of individual precursor and

spin coated at 2000 RPM with an acceleration of 500 for 45 seconds. The coated films were then annealed at 150 °C for 40 minutes under 30% RH.

SEM (Scanning Electron Microscopy) is the most crucial tools for the failure analysis. It includes the surface analysis like the surface morphology, roughness, cracks etc. Here it was performed to check the surface topology and composition of the respective films.

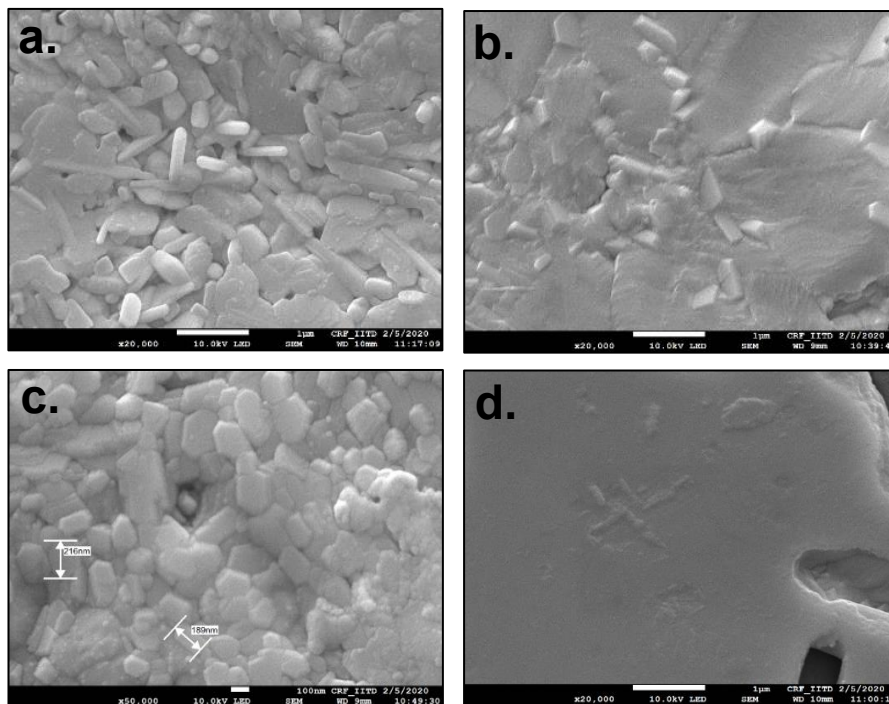


**Figure 33.** SEM of perovskite films

The figure 33, above clearly shows a smoother surface accompanied by the large size grain for  $\text{PbCl}_2$  (d) film while the other perovskite films formed through HCl (a), FAcI (b) and MACl (c) have a small grain size with a rough surface. So here we can say that a smooth grain signifies a better charge transfer properties if chlorine comes through  $\text{PbCl}_2$  than the coming from MACl, FAcI or HCl proving a better optoelectronic properties for the former perovskite film formed .



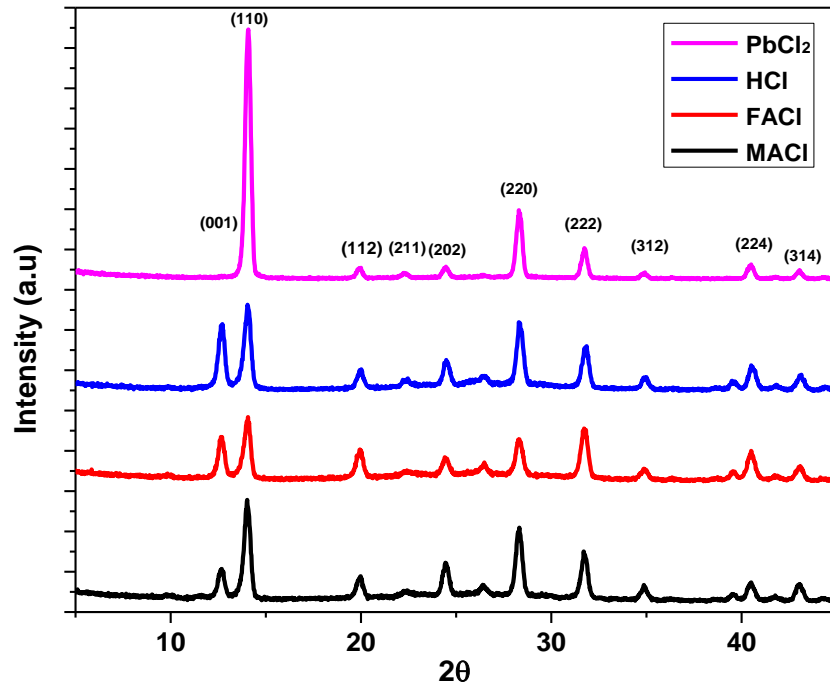


**Figure 34.** XRD plot

Figure 34, shows that the perovskite is formed along with the  $\text{PbI}_2$  phase except for the  $\text{PbCl}_2$ . And the  $\text{PbI}_2$  phase formed at (12.58 degree) dominates the perovskite phase formed at (28.4 degrees) as the perovskite formed breaks down to  $\text{PbI}_2$ . Furthermore, the peaks at 14 and 28 degrees at 2 theta ( $2\theta$ ) values concluded that the perovskite ( $\text{FACsPbI}_3$ ) phase is formed in all the cases irrespective from where the chloride is introduced into the precursor. The XRD peak intensity for the  $\text{PbCl}_2$  films were high representing a crystalline film formation. And the  $\text{PbI}_2$  phase is negligible indicating the stability of the film. While in the other films formed, XRD peak intensity were respectively lower that the  $\text{PbCl}_2$  film. This shows that the films were not crystalline and the  $\text{PbI}_2$  phase which is responsible for film degradation is high. Hence we can say the latter mentioned films formed had lesser stability.

UV-Vis spectroscopy is the study of the interaction of light with the semiconducting material provides information regarding the further applicability of the materials on various experimental conditions. The UV-Vis spectroscopy is also another technique that have been used extensively to study the opto- electronic properties of perovskite. It is concerned regarding the absorption near the visible region of the spectra. The different UV-Vis curves seen in figure 35, shows a maximum absorption when chloride

is introduced through  $\text{PbCl}_2$ . The absorption range for the other perovskite precursors through which chloride is injected has a negligible difference.

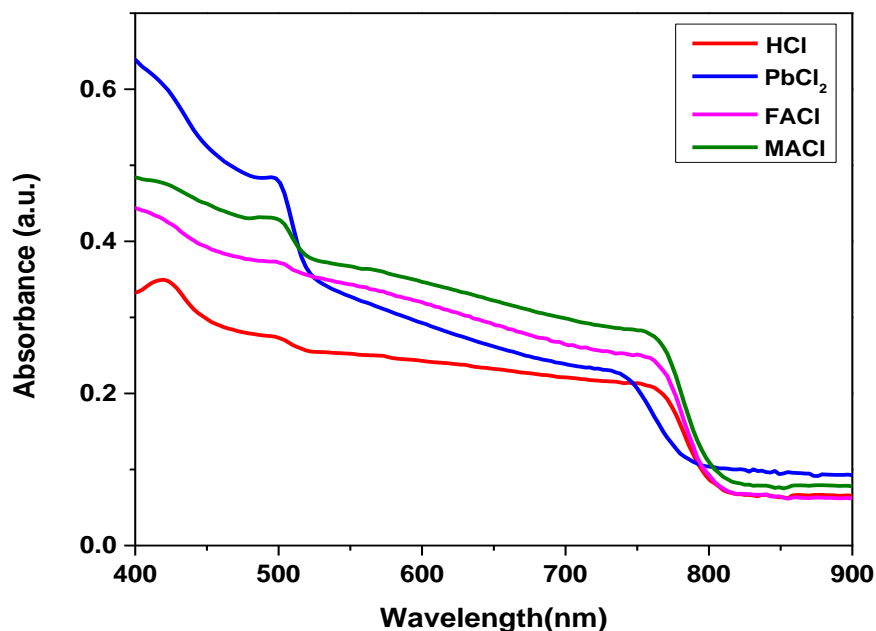


**Figure 35.** UV-Vis absorption in the visible region

EDX is an x-ray technique which used to determine the elemental composition of the material. In order to verify the products formed after the film formation. We conclude that the chlorine introduced is evaporated during annealing time. This confirms that the chlorine just helps in the passivation of the defect states and there is no traces left of chlorine in the final product of the perovskite i.e.  $\text{FACsPbI}_3$ .

Element	Weight%	Atomic%
C K	5.27	26.64
N K	3.15	13.65
O K	6.47	24.58
Cl K	0.00	0.00
I L	54.88	26.27
Pb M	30.23	8.86
Totals	100.00	

Element	Weight%	Atomic%
C K	5.90	26.04
N K	3.09	11.68
O K	9.99	33.10
Cl K	0.00	0.00
I L	52.19	21.80
Pb M	28.83	7.38
Totals	100.00	

Element	Weight%	Atomic%
C K	5.32	27.10
N K	3.18	13.89
O K	6.09	23.29
Cl K	0.00	0.00
I L	52.52	25.33
Cs L	4.07	1.87
Pb M	28.83	8.52
Totals	100.00	

Element	Weight%	Atomic%
C K	4.90	26.18
N K	1.13	5.17
O K	7.88	31.58
Cl K	0.00	0.00
I L	48.72	24.62
Cs L	5.10	2.46
Pb M	32.27	9.99
Totals	100.00	

**Table 3.** Elemental analysis of the perovskite films

**4.2.3: Device fabrication:** The fabrication of perovskite solar cells were done on fluorine-doped tin oxide (FTO) - coated glass substrates which has the resistance of approximately  $7 \Omega \text{ cm}^{-2}$ . The FTO glass substrates were patterned and etched with Zn-power and 2M aqueous HCl (37%) followed by cleaning sequentially in soap water, deionized water, acetone, and IPA. After oxygen plasma treatment (which removes organic components) from FTO surface, a compact  $\text{TiO}_2$  layer (electron transport layer) was deposited by spin coating. The step-by-step sintering of the thin films were done at  $100^\circ\text{C}$ ,  $200^\circ\text{C}$ ,  $300^\circ\text{C}$ , and  $500^\circ\text{C}$  for 10 minutes, 15 minutes, 15 minutes and 30 minutes respectively on a ramped hot plate. The four different precursors were used as a perovskite layer and deposited on the top of c-  $\text{TiO}_2$  coated FTO substrate by spin-coating technique. During spin coating (last 10 sec), anisole ( $50 \mu\text{L}$ ) was dripped on the active layer. The FACs $\text{PbI}_3$  coated films were heated for 30 minutes at  $150^\circ\text{C}$  under ambient condition (30% RH). Afterwards, 10wt% Spiro- OMeTAD in chlorobenzene doped with LiTFSI as hole transport material (HTM) layer was coated by a spin- coating process on the top of perovskite coated FTO. The devices were then kept in a desiccator for ~20 hours having oxygen rich environment. Lastly, a 150 nm thick silver contacts which served as the top electrode were deposited through a shadow mask by vacuum thermal vapour deposition technique ( $10^{-7}$  Torr at rate of 0.2 nm/s) with an active area of  $0.1 \text{ cm}^2$ .

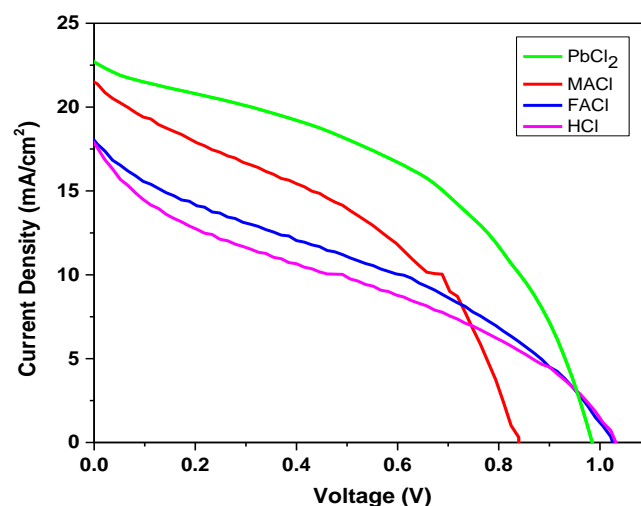


**Figure 36.** J-V Curve

Figure 36 shows the current – voltage (J-V) characteristics measured under simulated condition preferring AM 1.5G irradiation for champion device comprising of FTO / c-  $\text{TiO}_2$  / FACs $\text{PbI}_3$  / Spiro OMeTAD / Au. The device in which chlorine is introduced from

lead displayed the short circuit current density of 22.7 mA/cm<sup>2</sup>, fill factor of 0.48 or 48%, leading to highest PCE of 10.6%.

**Photovoltaic parameters derived from *J-V* measurements**

<b>Voc (V)</b>	0.98
<b>Jsc (mA/cm<sup>2</sup>)</b>	22.7
<b>Fill Factor (%)</b>	47.7
<b>Efficiency</b>	10.6%

**Table 4.**

<b>Voc (V)</b>	0.84
<b>Jsc (mA/cm<sup>2</sup>)</b>	21.5
<b>Fill Factor (%)</b>	42.4
<b>Efficiency</b>	7.6%

**Table 5.**

<b>Voc (V)</b>	1.01
<b>Jsc (mA/cm<sup>2</sup>)</b>	18.06
<b>Fill Factor (%)</b>	33.41
<b>Efficiency</b>	6.14%

**Table 6.**

<b>Voc (V)</b>	1.02
<b>Jsc (mA/cm<sup>2</sup>)</b>	17.8
<b>Fill Factor (%)</b>	29.2
<b>Efficiency</b>	5.34%

**Table 7.**

The table 4, 5, 6 and 7 shows the photovoltaic parameters of the devices in which lead is coming from PbCl<sub>2</sub>, MACl, FACl and HCl respectively. The maximum efficiency is displayed by PbCl<sub>2</sub> (table 4) devices followed by MACl, FACl and HCl.

## CONCLUSION

Firstly, the device fabrication with the  $\text{MAPbI}_3$  and  $\text{FACsPb}(\text{I}_{0.83}\text{Br}_{0.17})_3$  were done robustly. In order to perceive the Photovoltaic Performance the I-V testing were carried out and after stages of modification and optimization an efficiency of 5.24% and 12% were achieved for  $\text{MAPbI}_3$  and  $\text{FACsPb}(\text{I}_{0.83}\text{Br}_{0.17})_3$  devices respectively. In the other half of the project we have developed Chloride assisted perovskite precursor with  $\text{MACl}$ ,  $\text{FACl}$ ,  $\text{HCl}$  and  $\text{PbCl}_2$  followed by the thin film synthesis through the spin coating method to develop an efficient device. It was reported that the chloride presence in the perovskite is vital but as to where it should be added was not been leased. During the perovskite annealing process, chloride is immediately removed from the lattice to form a  $\text{FACsPbI}_3$  perovskite film. The addition of chloride through lead initiates a smooth-larger size grain film with negligible pin holes for hindrance to the charges to conduct. Whereas, a rough- flower shaped grains were observed in the other cases where chloride was added through the above mentioned salts into the perovskite precursor. These films initially formed  $\text{FACsPbI}_3$  which was decomposed to  $\text{PbI}_2$  with no chlorine traces in the lattice. In the photoluminescence spectroscopy the films formed by assisting  $\text{MACl}$ ,  $\text{FACl}$  and  $\text{HCl}$  supported the information of having a low PL intensity which suggests the presence of non-radiative recombination. This indicated the presence of defect states that might result in the loss of our charges. On the contrary, the films formed by assisting Chlorine via lead shows a radiative recombination supporting the presence of less defect states in the energy levels which can even be seen through the red shift of the peak for  $\text{PbCl}_2$  films. In XRD of the greyish film formed exhibited the strong peaks at  $14^\circ$  and  $28^\circ$  indicating the perovskite is formed. The result suggested that the films for  $\text{PbCl}_2$  were crystalline. Further the device fabrication were done by using these different perovskite precursor solution and it was found that the device in which chlorine is introduced from lead in the perovskite precursor has the highest efficiency of 10.6% among all.

## REFERENCES

1. Goetzberger A, J. Knobloch, and B. Voss, Crystalline silicon solar cell. *Editorial John Wiley & Sons Ltd*, **1998**
2. Keiichiro Masuko ; Masato Shigematsu ; Taiki Hashiguchi ; Daisuke Fujishima. Achievement of More Than 25% Conversion efficiency with crystalline silicon heterojunctionsSolar cell. *IEEE Journal of Photovoltaics*, **2016**, 1433 – 1435
3. A Kojima, K Teshima, Y Shirai, T Miyasaka, Organometal halide perovskites as visible light sensitizers for photovoltaic cells. *Journal of the American Chemical Society* 131 (17), **2009**, 6050-6051
4. NREL cell efficiency chart | Link: <https://www.nrel.gov/pv/cell-efficiency.html>
5. MA Green, A Ho-Baillie, HJ Snaith, *Nature Photonics* 8 (7), **2014**, 506
6. Yang, C.J., Reconsidering solar grid parity, *Energy policy*, **2010**, 38(7), 3270-3273
7. Kazmerski, L., D. Gwinner, and A. Hicks, *Best research cell efficiencies*, National Renewable Energy Laboratory, **2010**, 2, 0.0-2.0
8. Green, M.A., et al., *Solar cell efficiency tables (version 25)*, *Progress in photovoltaics*, **2005**, 13(1), 49-54
9. Shockley, W. and H.J. Queisser, Detailed balance limit of efficiency of p-n junction solar cells, *Journal of Applied Physics*, **1961**, 32(3), 510-519
10. Ray, S., S. De, and A. Barua, Characterization of microcrystalline silicon films prepared by the glow discharge method under different deposition conditions, *Thin Solid Films*, **1988**, 156(2), 277-286
11. Sastry, O., et al., Defect analysis in polycrystalline silicon solar cells, *Journal of Applied Physics*, **1985**, 57(12), 5506-5511
12. Carlson, D.E. and C.R. Wronski, Amorphous silicon solar cell. *Applied Physics Letters*, **1976**, 28(11), 671-673

13. Song, Y. and W. Anderson, Amorphous silicon/p-type crystalline silicon heterojunction solar cells with a microcrystalline silicon buffer layer, *Solar energy materials and solar cells*, **2000**, 64(3), 241-249
14. Britt, J. and C. Ferekides, Thin-film CdS/CdTe solar cell with 15.8% efficiency, *Applied Physics Letters*, **1993**, 62(22), 2851-2852
15. Olson, J., et al., A 27.3% efficient Ga<sub>0.5</sub>In<sub>0.5</sub>P/GaAs tandem solar cell, *Applied physics letters*, **1990**, 56(7), 623-625
16. Sites, J.R. and X. Liu, Recent efficiency gains for CdTe and CuIn<sub>1-x</sub>Ga<sub>x</sub>Se<sub>2</sub> solar cells, *Solar energy materials and solar cells*, **1996**, 41, 373-379
17. Schäfer, S., et al., Influence of the indium tin oxide/organic interface on open-circuit voltage, recombination, and cell degradation in organic small-molecule solar cells, *Physical Review B*, **2011**, 83(16), 165311
18. SD Stranks, HJ Snaith, Metal halide perovskites for photovoltaic and light emitting devices, *Nature Nanotechnology*, **2016**, 10(5), 391
19. HJ. Snaith, Perovskites: the emergence of a new era for low cost, high efficiency solar cells, *The journal of physical chemistry letters*, **2013**, 4(21), 3622-3630
20. Khagendra P Bhandari, Randy J. Ellingson, An overview of hybrid organic-inorganic metal halide perovskite, *Perovskite Photovoltaics*, **2018**
21. Green MA, Ho-Baillie A, Snaith HJ. The emergence of perovskite solar cells. *Nature Photonics*. **2014**, 8, 506-14
22. A Tumuluri, KL Naidu, KCJ Raju, Band gap determination using Tauc's plot for thin films, *Int. J. Chem. Tech*, **2014**, 6(6), 3353-3356
23. Murad JY Tayebjee, Louise C Hirst, NJ Ekins-Daukes, Timothy W Schmidt, The efficiency limit of solar cells with molecular absorbers: A master class approach, *Journal of Applied Physics*, **2010**, 108(12), 124506
24. Zhao, Y., A.M. Nardes, and K. Zhu, Solid-State Mesostructured Perovskite CH<sub>3</sub>NH<sub>3</sub>PbI<sub>3</sub> Solar Cells: Charge Transport, Recombination, and Diffusion Length. *Journal of Physical Chemistry Letters*, **2014**, 5(3), 490-494

25. Stranks, S.D., et al., Electron-Hole Diffusion Lengths Exceeding 1 Micrometer in an Organometal Trihalide Perovskite Absorber. *Science*, **2013**, 342(6156), 341-344
26. La-o-vorakiat et al., Elucidating the role of disorder and free-carrier recombination kinetics in CH<sub>3</sub>NH<sub>3</sub>PbI<sub>3</sub> perovskite films. *Nature Communication*, **2015**, 6
27. Stoumpos, C.C., C.D. Malliakas, and M.G. Kanatzidis, Semiconducting Tin and Lead Iodide Perovskites with Organic Cations: Phase Transitions, High Mobilities, and NearInfrared Photoluminescent Properties. *Inorganic Chemistry*, **2013**, 52(15), 9019-9038
28. Jacob Wilson, Jarvist M. Frost, Suzanne K. Wallace, and Aron Walsh, Dielectric and ferroic properties of metal halide perovskites, *APL Materials* **7**, **2019**, 10.1063/1.5079633
29. L. F. Vassamillet and V. E. Caldwell, Electron-Probe Microanalysis of Alkali Metals in Glasses, *Journal of Applied Physics*, **2003**, 1637 (1969)
30. John P. Sibilis, A Guide to Materials Characterization and Chemical Analysis, *J. Am. Chem. Soc.*, **1998**, 120, 37, 9728-9728
31. David Brandon, Wayne D. Kaplan, Microstructural Characterization of Materials, *John–Wiley and Sons*, **1999**
32. Mario Alejandro Mejía Escobar, Sandeep Pathak, Jiwei Liu, Henry J. Snaith, Franklin Jaramillo. *ACS Appl. Mater. Interfaces*, **2017**, 2342-2349
33. Xiangnan Bu, Robert Westbrook, Luis Lanzetta, Dong Ding, and Saif Haque. Surface Passivation of Perovskite Films via Iodide Salt Coatings for Enhanced Stability of Organic Lead Halide PSCs. *Sol. RRL*, **2018**, 1800282
34. Michael Saliba, Juan-Pablo Correa-Baena, Martin Stollerfoht, Nga Phung, Antonio Abate. How to Make over 20% Efficient PSCs in Regular and Inverted Architectures. *Chem. Mater*, **2018**, 30, 13, 4193-4201
35. Priyanka Chhillar, Bhanu Dhamaniya, Viresh Dutta, Sandeep K. Pathak. Recycling of Perovskite Films: Route toward Cost-Efficient and Environment-Friendly Perovskite Technology, *ACS Omega*, **2019**, 4, 7, 11880-11887



36. Javier Urieta, Ines Garcia-Benito, Agustin Molina-Ontoria and Nazario Martin, Hole transporting materials for perovskite solar cells: a chemical approach, *Chemical society review*, 2018, issue 23
37. HJ Snaith, how should you measure your solar cells, *Energy and environmental science*, **2012**
38. Boyuan Qi, Jizheng Wang, Open-circuit voltage in organic solar cells, *Journal of materials chemistry*, **2016**, issue 46
39. Johannes Greulich, Markus Glatthaar, Stefan Rein, Fill factor analysis of solar cells' current-voltage curves, *Wiley online library*, **2010**, 18(7)
40. Michael Saliba, Juan-Pablo Correa-Baena, Christian M. Wolff, Martin Stollerfoht, Nga Phung, Steve Albrecht, Dieter Neher and Antonio Abate, How to Make over 20% Efficient Perovskite Solar Cells in Regular (n-i-p) and Inverted (p-i-n) Architectures, *Chem. Mater.* **2018**, 30, 13, 4193-4201